Endothelial Targeting of Antibody-Decorated Polymeric Filomicelles

Vladimir V. Shuvaev,[†] Marc A. Ilies,[†,⊥] Eric Simone,[†] Sergei Zaitsev,[†] Younghoon Kim,[‡] Shenshen Cai,[‡] Abdullah Mahmud,[‡] Thomas Dziubla,[§] Silvia Muro,[†] Dennis E. Discher,[‡] and Vladimir R. Muzykantov[†,*]

[†]Institute for Translational Medicine & Therapeutics and Department of Pharmacology, University of Pennsylvania School of Medicine, Philadelphia, Pennsylvania 19104-5158, United States, [‡]Department of Chemical and Molecular Engineering, University of Pennsylvania School of Engineering and Applied Sciences, Philadelphia, Pennsylvania 19104-6391, United States, [§]Department of Chemical and Materials Engineering, University of Kentucky, Lexington, Kentucky 40504-0046, United States, and [⊥]Department of Pharmaceutical Sciences, Temple University School of Pharmacy, Philadelphia, Pennsylvania 19140-5101, United States

ABSTRACT The endothelial lining of the lumen of blood vessels is a key therapeutic target for many human diseases. Polymeric filomicelles that self-assemble from polyethylene oxide (PEO)-based diblock copolymers are long and flexible rather than small or rigid, can be loaded with drugs, and—most importantly—they circulate for a prolonged period of time in the bloodstream due in part to flow alignment. Filomicelles seem promising for targeted drug delivery to endothelial cells because they can in principle adhere strongly, length-wise to specific cell surface determinants. In order to achieve such a goal of vascular drug delivery, two fundamental questions needed to be addressed: (i) whether these supramolecular filomicelles retain structural integrity and dynamic flexibility after attachment of targeting molecules such as antibodies, and (ii) whether the avidity of antibody-carrying filomicelles is sufficient to anchor the carrier to the endothelial surface despite the effects of flow that oppose adhesive interactions. Here we make targeted filomicelles that bear antibodies which recognize distinct endothelial surface molecules. We characterize these antibody targeted filomicelles and prove that (i) they retain structural integrity and dynamic flexibility and (ii) they adhere to endothelium with high specificity both *in vitro* and *in vivo*. These results provide the basis for a new drug delivery approach employing antibody-targeted filomicelles that circulate for a prolonged time yet bind to endothelial cells in vascular beds expressing select markers.

KEYWORDS: nanoparticle · filomicelle · drug targeting · drug delivery system · endothelial delivery

Endothelial cells line the luminal surfaces of blood vessels and represent an important therapeutic site for treating a plethora of diseases, ranging from cardiovascular and pulmonary to neurological diseases and cancer.[1−5] The targeting of drugs and imaging agents to endothelial cells can be challenging in part because flow transports blood components including drug carriers at roughly 10 endothelial cell lengths per second in capillaries, but targeting also holds great promise in the optimization of numerous medical interventions.[6−10] After intravenous injection, for example, drugs and drug carriers conjugated with antibodies to endothelial surface molecules platelet-endothelial cell adhesion molecule-1 (PECAM) and intracellular adhesion molecule-1 (ICAM) bind to the endothelium and accumulate in vascularized organs, especially in the pulmonary vasculature.[11−14] The lung represents a major fraction of the endothelial surface and is perfused by 100% of cardiac venous blood output. Therefore, circulating antibodies to these and other endothelial surface determinants accumulate in the lung.[9,15] Endothelial immunotargeting enhances the efficacy and specificity of therapeutic action of diverse drugs in animal models of thrombosis, ischemia, lysosomal storage diseases, and inflammation.[11,13,16−20] Endothelial drug delivery (vascular immunotargeting) thus represents a translational goal of broad importance.

One particularly intriguing, but poorly defined, aspect of targeted drug delivery is the affinity features of carriers of diverse shapes that have become recently available.[21−24] The carrier geometry modulates circulation and interactions with cells.[14,25−28] For example, elongated carriers have shown longer circulation compared to spherical counterparts, thereby improving bioavailability and pharmacological effects.[29,30] To date, the knowledge of the role of carrier geometry in endothelial targeting is limited to one comparison of spheroid and discoid polystyrene particles targeted to ICAM-1; while the latter carrier showed higher efficacy and specificity of targeting,[14] similar studies have not been pursued with other shapes or compositions.

In this context, polymeric filomicelles, a novel type of drug carriers based on amphiphilic diblock copolymers containing as a hydrophilic portion polyethylene oxide (PEO, or polyethylene glycol, PEG) that can be loaded with diverse drugs and contrast agents for imaging, are of particular interest.[29,30] Polymeric filomicelles are flexible elongated supramolecular structures self-assembled

* Address correspondence to muzykant@mail.med.upenn.edu.

Received for review April 27, 2011 and accepted August 13, 2011.

Published online August 13, 2011
10.1021/nn2015453

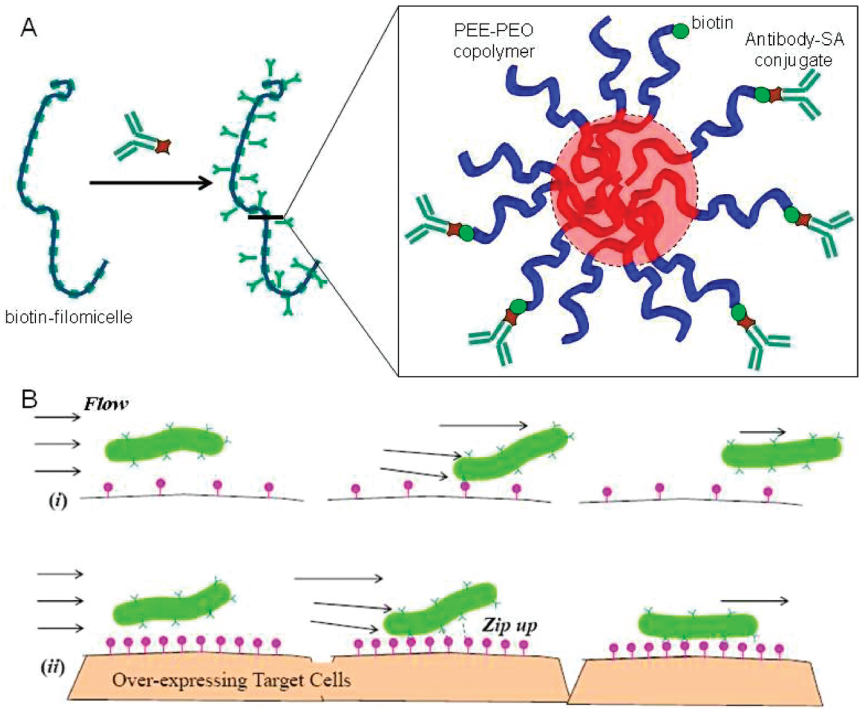

Figure 1. Design of antibody-decorated filomicelles (Ab/filomicelles) and proposed mechanism of their anchoring to the target endothelial cells under blood flow. (A) Left top panel shows a general schematic view of biotinylated and antibody-coated filomicelles (Ab/filomicelle); inset shows cross section of the Ab/filomicelle with highlighted hydrophobic area (red area) loaded with hydrophobic therapeutic or imaging agents (*e.g.*, red fluorescent probe PKH-26 in the present study). Biotin residues (green spheres) covalently conjugated to the free end group of the PEO part of the PEE-PEO diblock copolymer (PEE block in red and PEO block in blue). Biotin-copolymer is blended to pristine copolymer prior to filomicelles formation, providing biotin residues exposed in the PEO corona used for subsequent attachment of covalent antibody−streptavidin (SA) conjugates (green Y-like symbols indicate antibody, and brown squares indicate streptavidin) to biotin-filomicelles. (B) Targeting of a long and flexible filament in blood flow. (*i*) If the filomicelle avidity (dictated by affinity of attached antibody and its surface density on the filomicelle) or expression of endothelial binding sites is below the critical level, then shear forces—which increase with particle length *L*—will dominate and prevent anchoring of the filament. (*ii*) If the filomicelle avidity and target site density on the endothelium are sufficiently high, then binding prevails and the filament "zips up" on the targeted cell despite the flow.

from stealthy diblock copolymers, which have extremely high aspect ratio (20−60 nm in diameter and 1−20 μm in length).[29] Due to such a high aspect ratio and, when above the glass transition temperature, their structural flexibility, filomicelles align with flow, meander around obstacles including cells and avoid cellular uptake.[29,31] As a result of these unique hydrodynamic and stealth features endowed by PEO corona, filomicelles have a uniquely long lifetime in circulation, representing attractive nanocarriers for vascular drug delivery, and initial studies have indicated that circulating filomicelles can deliver drugs to tumors.[29]

Antibody-based targeting of filomicelles is studied in the present work. Despite the exciting potential of filomicelles to serve as carriers for targeted drug delivery, two key aspects of their nature, both fundamental for this function, have not been addressed. First, it is unclear whether self-assembled supramolecular filomicelles retain structural integrity and dynamic flexibility after attachment of a sufficient number of a relatively large targeting molecule such as an antibody. Second, it is also unclear whether the avidity of antibody-bearing filomicelles is sufficient to anchor the carrier to the endothelial surface despite the effects of flow that impair adhesive interactions with vascular cells. Here we generated filomicelles carrying various antibodies that recognize a range of endothelial surface molecules and found that these carriers exert highly specific endothelial targeting in both cell cultures and animals after intravenous injection.

RESULTS AND DISCUSSION

Synthesis of the Filomicelles. We devised a one-step attachment of covalent streptavidin−antibody conjugates to filomicelles containing biotinylated copolymer (Figure 1). The $(EO)_3$ linker ((+)-biotinyl-3,6,9-trioxaundecanediamine) used to synthesize biotinylated diblock copolymers provides biotin exposure in the hydrophilic corona of the resultant filomicelles and optimum length for both efficient streptavidin binding and high conjugating reactivity (low steric hindrance of the amino group). Synthesis in an excess of amine provided biotin-poly(ethylethylene)-*b*-poly(ethyleneoxide) (PEE_{37}-PEO_{40}-OCONH-$(EO)_3$-CH_2CH_2NH-biotin, biotin-OE7) and biotin-poly(butadiene)-*b*-poly(ethyleneoxide) (PBD_{125}-PEO_{79}-OCONH-$(EO)_3$-CH_2CH_2NH-biotin, biotin-OB18) with

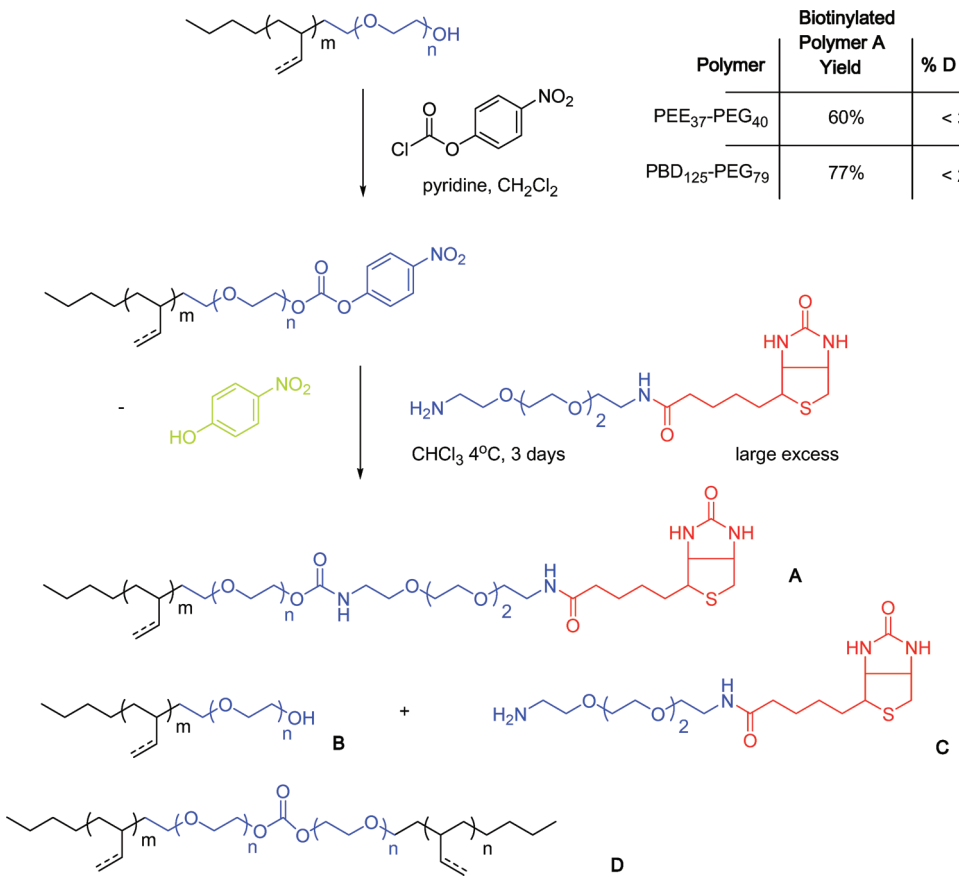

Polymer	Biotinylated Polymer A Yield	% D (GPC)
PEE_{37}-PEG_{40}	60%	< 3 %
PBD_{125}-PEG_{79}	77%	< 2 %

Figure 2. Optimized synthetic scheme for biotinylated diblock copolymers OE-7 (PEE_{37}-PEO_{40}) and OB-18 (PBD_{125}-PEO_{79}). Synthetic conditions and purification strategy allow the generation of biotinylated diblock copolymer (A) with good yield and low impurity levels of initial OB-18 (B) and biotin-PEG_3-NH_2 (C) and byproduct OB-18 self-reaction producing triblock copolymer (D). Inset: table shows obtained yield of diblock copolymer A (weight percentage) and fraction of triblock copolymer D determined by GPC (weight percentage). More detailed explanation and additional data are given in Supporting Information.

minimal contamination of dimer and other side products (Figure 2; see Supporting Information for details). Excess biotin-$(EO)_3$-NH_2 was removed through several washings with dilute aqueous citric acid. GPC analysis showed that the coupling of two molecules of activated diblock copolymers yielded less than 3% of the unwanted triblock copolymers (Figure 2, inset table). ^{1}H NMR revealed a characteristic 4.15 ppm signal in the biotinylated copolymers (Supporting Information, Figure S1a,b, peak "c"), representing the terminal ethylene unit of the parent polymer. This signal was up-shifted from the initial position of 3.7−3.8 ppm due to the replacement of the attached OH group with the more deshielding carbamate group formed by conjugation of biotin-$(EO)_3$-NHCO- in the biotinylated polymer.

The biotinylated copolymer was blended with nonmodified copolymer at different ratios, and the polymer mixtures were hydrated to generate the biotinylated filomicelles. Their morphology and length were characterized by fluorescence microscopy. In accord with previous studies,[29] the average length of filomicelles formulated using nonbiotinylated OE-7 diblock copolymer was 15 μm (Figure 3), and it should be noted that the polydispersity in length is typically a few micrometers. Filomicelles displayed a high degree of flexibility that can be seen in Supporting Information video. Blending the nonbiotinylated copolymer with biotinylated OE-7 resulted in gradual reduction of the contour length of the resultant filomicelles, to 50% of the initial length (7−7.5 μm) at 4 mol % biotinylated polymer in the blend. This effect can be attributed to the increase of the average hydrophilic part of the diblock copolymer blend as compared with the nonbiotinylated polymer (the biotin-OE7 polymer is more hydrophilic than parent EO7 due to extra EO units brought by the biotin linker and to the intrinsic polarity of the biotin moiety). The addition of biotin-OE7 in the blend above 4 mol % did not further shorten filomicelles but led to progressive contamination of filomicelles by spherical micelles. Furthermore, large amounts of polymersomes (20−30%) were observed in the hydrated samples of biotin-OB18 diblock copolymer blends (not shown). To avoid these heterogeneities, we have focused on the filomicelles formed from OE7 copolymer blended with up to 4 mol % of biotin-OE7 copolymer.

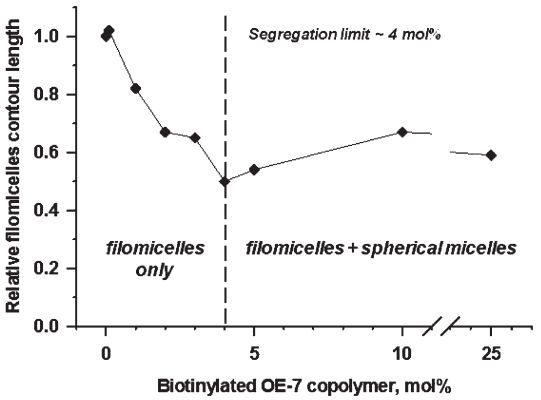

Figure 3. Effect of inclusion of biotinylated block copolymer on length of filomicelles. Influence of biotinylated block copolymer amount on the morphological characteristics of corresponding filomicelles obtained from its blends with nonbiotinylated block copolymer. The contour length of filomicelles decreases with the increase of the percentage of biotinylated copolymer in the blend. Blending of more than 4 mol % of biotinylated copolymer results in generation of spherical micelles mixed with filomicelles. Pristine (pure) OE filomicelles (length L = 15 μm, diameter D = 10 nm) without biotinylated copolymer was used as reference, and its relative contour length was considered as 1.0. Lines connect experimental points for presentation purpose only.

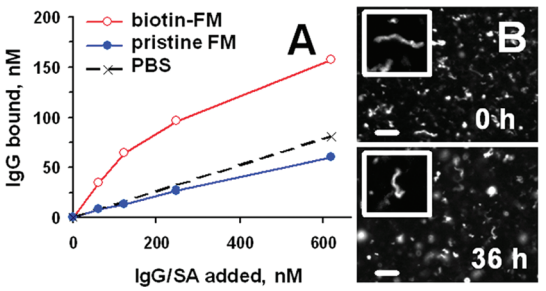

Figure 4. Synthesis of IgG-coated filomicelles. (A) ^{125}I-IgG/SA conjugation to biotin-filomicelles. ^{125}I-IgG/SA was incubated for 30 min at 20 °C with pristine PEO-PEE filomicelles *vs* filomicelles containing 4 mol % of biotin-PEO-PEE. Filtering through 0.22 μm pore Millipore filters retaining filomicelle-bound ^{125}I-IgG/SA revealed that ^{125}I-IgG/SA did not bind to pristine filomicelles, showing the same retention on the filter as after filtration of free ^{125}I-IgG/SA in PBS. PEO assay showed that 95% of filomicelles were retained on the filter. Note that the curve for pristine filomicelles coincides with the curve for PBS, reflecting some nonspecific binding of ^{125}I-IgG/SA to the filter. (B) Stability of IgG/filomicelles. IgG/SA was conjugated with biotinylated filomicelles (initial L ~10 μm) labeled with PKH26 fluorescent dye. Fluorescence microscopy revealed no apparent aggregation or degradation of IgG/filomicelles after incubation with fresh human plasma for 36 h at 37 °C. Scale bar: 10 μm. Bright fluorescent spheres represent moving filomicelles out of the focal plane. Lines connect experimental points for presentation purpose.

Coupling of Antibody–Streptavidin Conjugates to Filomicelles and Binding of Ab/Filomicelles to Endothelial Cells. Streptavidin–biotin approach for protein attachment to filomicelles allows (i) modular attachment of various antibodies or control IgG to the surface of polymeric filomicelles and (ii) adjustment of the antibody density *via* modulation of the biotinylated polymer ratio in the polymer blend. In order to avoid aggregation of biotinylated filomicelles by tetravalent streptavidin (SA), we used one-step attachment of covalent IgG/SA conjugates instead of two-step streptavidin-mediated attachment of biotinylated proteins. IgG/SA conjugates do not cause aggregation of biotinylated carriers since streptavidin–biotin binding sites in the conjugates are partially blocked by the IgG molecule and cannot accommodate more than one biotin residue conjugated to a macromolecule or nanocarriers.[18]

Using this approach, we attached IgG/SA or diverse Ab/SA to biotinylated filomicelles, producing IgG/SA-biotin-filomicelles and Ab/SA-biotin-filomicelles, indicated hereafter as IgG/filomicelles and Ab/filomicelles. In order to measure the number of IgG molecules attached to filomicelles and trace them in targeting studies *in vitro* and *in vivo*, ^{125}I-IgG/SA was mixed with nonlabeled IgG/SA or Ab/SA (in the case of nonspecific *versus* targeted filomicelles, respectively) at 1:9 ratio or 10 mol % of labeled conjugates. In a series of experiments, shown in Figure 4, we attached ~1600 copies of IgG/SA per average biotinylated filomicelle with 10 μm length (L) at maximal IgG/SA input (Figure.4A). The estimation was based on the calculated maximal binding of IgG/SA to biotinylated filomicelles of 625 molecules PEE-PEO per one molecule of IgG/SA (Figure 4A).

Filtration studies showed that IgG/SA attaches specifically to biotinylated but not pristine filomicelles (Figure 4A and Supporting Information Figure S3). Initial linear fragment of IgG/SA binding to biotinylated micelles (Figure 4A, open circles, 0–100 nM of IgG/SA) reflects strong interaction between IgG/SA and biotin, whereas fragment 100–600 nM IgG/SA goes in parallel with control curve (dashed lane) and reflects saturation of the biotinylated micelles with the SA conjugates. IgG/SA did not cause aggregation of biotinylated filomicelles and Ab/filomicelles retained structural integrity for at least 36 h incubation in fresh human plasma at 37 °C (Figure 4B).

Anti-PECAM/filomicelles bound to endothelial cells while retaining the distinctive shape and size of filomicelles as is easily discerned by fluorescence microscopy (Figure 5A). Quantitative analysis of ^{125}I-IgG/SA tracer attached to filomicelles showed that binding of anti-PECAM/filomicelles is specific, as control IgG/filomicelles showed very low binding (Figure 5B).

IgG/Filomicelles Have High Blood Level in Circulation and Low Retention in Capillaries. In the first series of *in vivo* experiments, we determined blood level and lung uptake of IgG/filomicelles after intravenous, tail-vein injection in mice, and we compared them to spherical and discoid IgG/carriers. We used formulations carrying nonspecific IgG to avoid potential confounding effects of targeting on parameters such as blood clearance and biodistribution of carriers. Cells such as macrophages in the liver and spleen possess receptors to bind the Fc portion of IgG, and so some extent of coated carrier

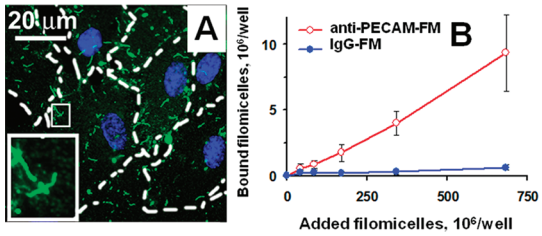

Figure 5. Binding of the anti-PECAM/filomicelles to endothelial cells. (A) Fluorescence micrographs (400×) of labeled anti-PECAM/filomicelles bound to cells. HUVEC were incubated for 1 h at 37 °C with labeled filomicelles, washed, and stained. The cell nuclei were stained with DAPI (blue). Dashed lines mark the cell borders, as observed by contrast phase. Inset: 4× magnified image of filomicelles bound to endothelial cells. (B) Quantification of binding of ^{125}I-traced filomicelles coated by IgG or anti-PECAM to HUVEC. Cells were incubated with increasing concentrations of radiolabeled filomicelles for 1 h at 37 °C, washed, lysed, and measured using a γ-counter. Mean ± SD values are shown, $n = 3$. Lines connect experimental points for presentation purpose.

TABLE 1. Level of ^{125}I-IgG/Carriers in Blood and Lungs after Intravenous Injection in Mice[a]

	IgG spheres	IgG filomicelles
blood, %ID[b]	6.2 ± 0.7[c]	38.1 ± 13.3
blood, %ID/g	3.6 ± 0.5	25.8 ± 9.0
lung, %ID/g	9.3 ± 2.4	4.7 ± 2.1
lung/blood LR	2.7 ± 0.7	0.2 ± 0.05

[a] Mice were injected *via* tail vein with IgG-conjugated formulations, and 1 h later, isotope level in blood and lungs was measured to calculate % of injected dose per gram of tissue (%ID/g). Blood represents ~7% of body weight, *i.e.*, ~1.5−1.8 g in adult 20−25 g in mice. [b] LR, localization ratio: %ID/g in an organ divided by %ID/g in blood. [c] The data are shown as mean ± SD, $n = 3$.

clearance is to be expected. Radiolabeled IgG/discs and IgG/filomicelles showed, respectively, 2-fold and 6-fold higher blood level than IgG/spheres (Table 1 for spheres and filomicelles; data for IgG/discs were published previously[14]). Distribution of IgG/carriers in the main organs 1 h after iv injection is shown in Supporting Information (Table S1). Therefore, elongated carriers, especially flexible filomicelles, are cleared from the bloodstream much less effectively than spherical carriers despite the much larger major dimension of the former carriers: discs and filomicelles are 3 and ~7.5 μm in length, respectively, whereas the mean diameter of spheres is ~150 nm.

Pulmonary uptake of IgG/filomicelles after 1 h was studied next and calculated as a localization ratio, LR, % ID/g in an organ divided by %ID/g in blood. For the IgG/filomicelles, LR was almost 14-fold lower than IgG/spheres (Table 1) and being nearly zero and is one of the lowest pulmonary uptake levels reported in the literature.[10,14] Furthermore, despite a major difference in maximal dimension, the asymmetric IgG/discs showed about 4-fold higher nonspecific vascular retention *versus* IgG/filomicelles. The measurements confirm that nontargeted filomicelles exert minimal nonspecific retention in a highly perfused organ such as lung with extended capillary networks. This result is of high translational value, as it implies that filomicelles do not cause vascular embolism and thereby supports potential clinical safety of these carrier (Table 1).

Table 1 shows that, opposite to other carriers, the major fraction of IgG/filomicelles (~40% of injected dose) remained in the circulation 1 h after iv injection. Blood represents ~30% of total mass of the lung, the most vascularized and perfused organ in the body. Therefore, the lung level of isotope after injection of IgG/filomicelles may largely reflect the residual blood pool in the pulmonary vessels. Indeed, infusion of 10 mL of PBS/heparin at sacrifice, providing bloodless white lungs, reduced pulmonary level of IgG/filomicelles by ~80% (4.7 ± 1.2 *vs* 1.1 ± 0.7 *vs* %ID/g in nonperfused *vs* perfused lungs). Therefore, 3.6% ID/g of the pulmonary uptake of IgG/filomicelles can be attributed to nonbound fraction in the residual blood pool in the pulmonary vasculature. Accordingly, this value is subtracted from data of pulmonary uptake of targeted Ab/filomicelles obtained in the subsequent experiments, in order to eliminate the nonspecific blood pool fraction (see below).

Endothelial Targeting of Antibody/Filomicelles *in Vivo*. To study endothelial targeting in animals, we measured pulmonary uptake of Ab/carriers after tail-vein injection into healthy mice. We used antibodies directed to endothelial surface molecules ICAM-1, PECAM-1, and thrombomodulin (two monoclonal antibodies: low affinity TM_{273} and high affinity TM_{411}). The Ab surface density was ~7000 and ~8000 Ab/μm^2 for spheres and filomicelles, respectively. Nonspecific IgG/filomicelles served as a control for background levels of nonspecific binding. For rigorous analysis of the specificity of the endothelial targeting manifested by pulmonary accumulation, we calculated the ratio of uptake of targeted filomicelles *versus* nontargeted formulation normalized by respective blood levels, that is, the immunospecificity index (ISI). This provides the most accurate measure of targeting specificity.[7]

Ab/spheres showed a higher level of pulmonary targeting than free antibodies, reflecting high avidity of this type of carrier. Both the absolute uptake in the lung expressed as %ID/g (Figure 6A) and targeting specificity expressed as immunospecificity index (Figure 6B) increased 2- and 3-fold with anti-ICAM/spheres and anti-TM/spheres relative to the respective free antibodies (non-carrier-conjugated). A notable exception was found with thrombomodulin antibody TM_{273}, which is known to have a relatively low affinity.[32−34]

In contrast to Ab/spheres, Ab/filomicelles showed lower absolute uptake in the lung than free antibodies (Figure 6A), including both the nonspecific IgG and the targeting antibodies. These results are fully consistent with the persistent circulation and enhanced stealth

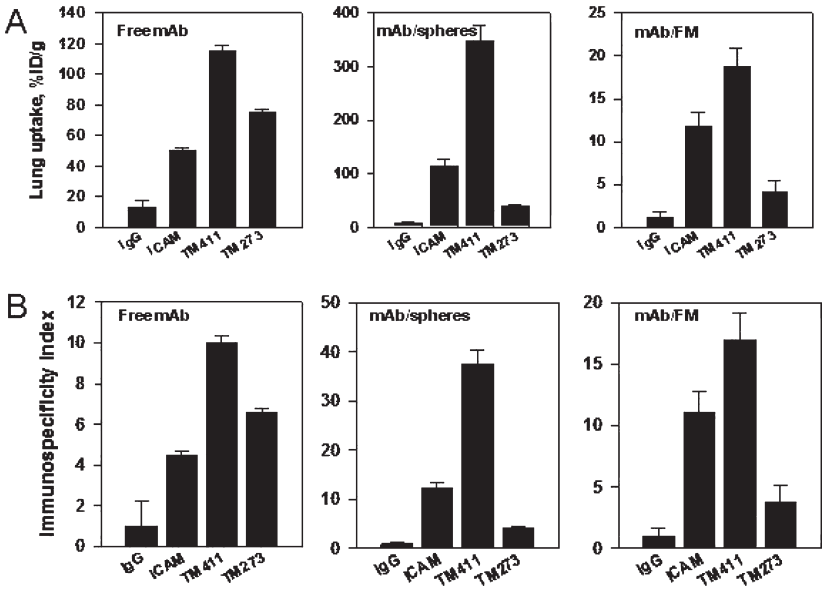

Figure 6. Pulmonary accumulation of targeted *vs* nontargeted filomicelles. (A) Data show levels of lung uptake of ^{125}I-traced formulations: nonconjugated antibodies (free mAb), coated spherical nanoparticles (mAb/spheres), and coated filomicelles (mAb/FM), 1 h after iv injection in mice. All differences in each panel are significant ($p < 0.05$, $n = 3$, mean ± SEM values are shown). Experimental conditions are described in Table 1. (B) ISI: %ID/g of mAb to %ID/g of IgG (*i.e.*, ISI of IgG-based formulation is always 1).

features of filomicelles as they avoid vascular collisions,[29] which thus inhibits rapid attachment of the carrier to target cells. However, the specificity for pulmonary uptake showed a similar ISI ~11−12 for anti-ICAM/filomicelles and anti-ICAM/spheres (Figure 6B), as well as a similarly suppressed ISI ~3−4 for both the lowest affinity TM_{273}/filomicelles and TM_{273}/spheres. These latter results with low affinity TM_{273} support the idea that the avidity of carriers bearing low affinity vectors is suboptimal for efficient anchoring to endothelial cells *in vivo*. Hydrodynamic drag forces drive detachment and prevent tight attachment of such carriers. The results thus are consistent with the important role of *in vivo* hydrodynamics both in the targeting ability and in sustained circulation of elongated filomicelles.

High affinity targeting of the TM_{411}/filomicelles considerably exceeds—as expected from arguments above—the ISI of free antibody. Additionally, pulmonary uptake of anti-PECAM/filomicelles was found to be 8.8 ± 0.7% ID/g (ISI = 8; not shown), which is similar to the results for targeting ICAM. Because ICAM-1, TM, and PECAM-1 have differential localizations (in the apical plasmalemma, lipid rafts, and intercellular contacts, respectively),[35] the results indicate that filomicelles can be targeted with high affinity antibodies to a wide variety of endothelial surface molecules localized in diverse plasmalemmal domains. Ab/filomicelles thus display a unique but robust capacity to circulate for a long-time while retaining high specificity for targets.

Results presented here demonstrate that it is possible to formulate stable and dynamically flexible polymeric filomicelles surface-decorated with a sufficient number of antibodies to avidly anchor onto target endothelial cells *in vivo* despite the opposing effect of blood flow. Filomicelles bearing nonspecific IgG display the highest blood levels and also the lowest nonspecific uptake (about 10-fold lower) in the vascularized organs *versus* IgG-coated spherical nanocarriers. This is likely due to flow alignment which inhibits carrier interactions with blood cells and vascular cells. Nonetheless, filomicelles with antibodies targeting diverse endothelial surface molecules exhibit avidity sufficient to overcome flow inhibition and then anchor Ab/filomicelles to the pulmonary endothelium. Filomicelle avidity is clearly regulated by affinity of the targeting antibodies—even when directed at the same antigen, as illustrated by thrombomodulin antibodies.

Taken all together, these results show that targeted Ab/filomicelles combine high stealth and persistent circulation with high avidity, thus representing a new class of nanocarriers for vascular drug delivery to select cell types. This approach holds promise to improve pharmacotherapy and alleviate adverse effects. For example, immune response to components of drug delivery systems represents an important and challenging problem. In this context, we believe that design of the carriers achieving therapeutic goals with lower dose and number of injections (*i.e.*, due to targeting and improved circulation) may help alleviate this concern.

In the present proof-of-principle study, we focused on the design of Ab/filomicelles and characterization of their binding to endothelium. Our results warrant imminent follow-up studies of drug release from and cellular uptake of Ab/filomicelles. The latter issue is of

the utmost importance and novelty, taking into account that internalization pathways conventionally accepted as prevalent in endothelial cells (clathrin and caveolar endocytosis) serve much smaller objects. However, cell adhesion molecule (CAM)-mediated endocytosis previously described by our team permits endothelial uptake of carriers with diameter up to few micrometers, on the condition that they bind to proper epitopes on ICAM-1 or PECAM-1.[14,36] Therefore, in theory, anti-CAM/filomicelles might enter this pathway, especially if a long filomicelle coils in the endosomes. We hope that the future studies will clarify this intriguing issue.

METHODS

Please refer to the Supporting Information for details.

Materials and Cell Cultures. The following reagents were used: chloroform, pyridine, ethanol, dichloromethane, citric acid from Fisher Scientific (Pittsburgh, PA), 4-NO_2-phenylchloroformate from Acros Organics (Morris Plains, NJ), PKH-26 dye from Sigma-Aldrich (St. Louis, MO), and HABA (4′-hydroxyazobenzene-2-carboxylic acid), 4-[*N*-maleimidomethyl]cyclohexane-1-carboxylate (SMCC), EZ-link amine-$(EO)_3$-biotin, that is, biotin-$(EO)_3$-amine ((+)-biotinyl-3,6,9-trioxaundecanediamine), NHS-LC-biotin (*i.e.*, succinimidyl-6-[biotinamido]hexanoate), *N*-succinimidyl-(*S*)-acetylthioacetate (SATA), and Iodogen from Pierce Biotechnology (Rockford, IL). Diblock copolymers poly(ethylethylene)-*b*-poly(ethyleneoxide) (PEE_{37}-PEO_{40}, OE-7) and poly(butadiene)-*b*-poly(ethyleneoxide) (PBD_{125}-PEO_{79}, OB-18) were described previously.[29] These particular polymers eliminate any possible confounding effects of chemical degradation in the studies below.

Nonspecific IgG was from Jackson Immuno-Research Laboratory, Inc. (West Grove, PA). Antibodies (Abs) to endothelial surface proteins PECAM-1, ICAM-1, and thrombomodulin have been described in our previous studies.[34] Antibodies to thrombomodulin were kindly provided by Dr. Stephen J. Kennel. For studies of spherical carriers, FITC-labeled polystyrene microspheres (0.1 μm diameter) from Polysciences (Warrington, PA) were coated with nonspecific ^{125}I-IgG or a mix of ^{125}I-IgG and nonlabeled specific antibody at 5:95 molar ratio, as we described.[14] For experiments of prototype targeted filomicelles, antibodies were covalently conjugated with streptavidin (SA) to form covalent IgG/SA or Ab/SA conjugates using SATA-SMCC chemistry as we described.[18,20] Proteins were radiolabeled with sodium iodide radioisotope Na^{125}I (PerkinElmer; Wellesley, MA) using Iodogen as we described.[37]

Human umbilical vein endothelial cells (HUVEC) were purchased from Clonetics (San Diego, CA). All cell culture medium components were from Life Technologies (Gaithersburg, MD) unless otherwise noted. Confluent cells were maintained in M199 medium (GIBCO, Grand Island, NY) with 15% fetal bovine serum supplemented with 100 μg/mL heparin (Sigma), 2 mM L-glutamine (GIBCO), 15 μg/mL endothelial cell growth supplement (Upstate, Lake Placid, NY), 100 U/mL penicillin, and 100 μg/mL streptomycin (GIBCO).

Synthesis of Biotinylated Diblock Copolymers. The terminal hydroxyl groups of diblock copolymers poly(ethylethylene)-*b*-poly(ethyleneoxide) OE-7 and poly(butadiene)-*b*-poly(ethyleneoxide) OB-18 were activated with p-NO_2-phenylchloroformate (NPCF) and conjugated without a catalyst with biotin-$(EO)_3$-NH_2 following a variation of a previously described synthetic strategy.[38,39] The synthetic scheme and all experimental details are presented in the Supporting Information. Pristine and biotinylated polymers were characterized by the nuclear magnetic resonance (NMR) spectra, gel permeation chromatography (GPC), and matrix-assisted laser desorption/ionization time-of-flight (MALDI-TOF) mass spectrometry (see Supporting Information for details of protocols, equipment, and analysis).

Assembly of Biotinylated Filomicelles, Coupling of IgG/Streptavidin, and Characterization of the Resultant Ab/Filomicelles. Biotinylated filomicelles were prepared as previously outlined.[38] Biotinylated polymer was then blended with pristine polymer, and filomicelles were made *via* the film casting/rehydration method.[29] Formed biotinylated filomicelles (b-filomicelles) were incubated for 30 min with IgG/SA conjugates, and unbound IgG/SA was removed from filomicelles using 0.22 μm filter unit (Ultrafree-MC, Millipore, Bedford, MA), while filomicelles were effectively retained on the filter. Preliminary experiments showed that 95% of filomicelles were retained on the filter. Filomicelles were stained with the lipophilic fluorescent dye PKH26 and imaged by with Nikon Eclipse TE2000-U fluorescence microscope, a 40× PlanApo objective, and filters optimized for red PKH26 fluorescence. Images were obtained with a Hamamatsu Orca-1 charge-coupled device camera and analyzed using ImageJ software (NIH). Contour lengths (length as measured along the filomicelle backbone) were determined *via* established methods.

Binding of Anti-PECAM/Filomicelles to Endothelial Cells. Anti-PECAM/filomicelles or IgG/filomicelles, both carrying 10% of radiolabeled SA/IgG, were incubated with HUVEC at 37 °C for 1 h; unbound materials were washed out and cells were lysed with lysis buffer (1% Triton X-100, 1.0 M NaOH). Using as a tracer ^{125}I-IgG/SA lacking endothelial affinity eliminates the likelihood of false positive targeting results caused by tracer detachment from filomicelles in cell culture and *in vivo* experiments. Bound radioactivity was measured using a Wallac 1470 Wizard γ-counter (Gaithersburg, MD). In a parallel experiment, fluorescently labeled filomicelles were identified in HUVEC using the instruments described above for fluorescent microscopy. To facilitate visualization, filomicelle micrographs were pseudocolored in green using ImagePro 3.0 software (Media Cybernetics, Inc., Bethesda, MD), cell nuclei were stained with blue fluorescent DAPI, and the cell borders were identified by phase contrast. Our preliminary data showed that at a filomicelle concentration of 1.25 μM PEE-PEO maximal binding of IgG/SA was 2 nM; that is, one molecule of IgG was bound per 625 molecules of PEE-PEO. Corresponding ratio was used throughout the study to keep maximal coating. Our further calculations are based on the assumption that filomicelle diameter is D_{fm} = 20 nm and square area occupied by one polymer molecule on the filomicelle surface is $a_{polymer}$ = 0.62 nm^2. Thus, to estimate number of IgG/SA conjugated to filomicelles, we used calculated number of ~100 000 molecules of PEE-PEO packed per 1 μm of filomicelle length.

Pulmonary Uptake and Blood Level of Antibody-Coated Filomicelles *in Vivo*. Animal studies were performed according to a protocol approved by the Institutional Animal Care and Use Committee (IACUC) of the University of Pennsylvania. Filomicelles were coated with IgG/SA that included 10 mol % of radiolabeled IgG/SA, and 100 μg of prepared carrier was injected intravenously (iv) in C57BL/6J mice (The Jackson Laboratory, Bar Harbor, ME). After 1 h, animals were sacrificed and isotope level in tissues was determined in a γ-counter to calculate % of injected dose per gram of organ (%ID/g). Immunospecificity index (ISI), a parameter that better reflects targeting specificity, was calculated as %ID/g of Ab/filomicelles normalized per blood level and divided by same parameter of control IgG/filomicelles. Detailed explanation of these quantitative parameters is given elsewhere.[40]

Statistical Analysis. Unless specified otherwise, the data have been calculated and presented as mean and standard deviation (SD). Statistical difference among groups was determined by Student *t*-test and was accepted as significant at $p < 0.05$.

Acknowledgment. This study is supported by RO1 HL073940 and HL087036 (V.R.M.), R01 EB_{007049} (D.E.D.), Penn-CHOP CTSA and NSERC Fellowship (A.M.). Support of NRSA through a Fellowship in Cancer Pharmacology (M.A.I.) is gratefully acknowledged.

Authors are grateful to Dr. Samir Mitragotri, Department of Chemical Engineering, University of California, Santa Barbara, CA, for helpful discussions and providing IgG/discs.

Supporting Information Available: Video of 4 mol % filomicelles, additional detailed description of materials, methods, and figures. This material is available free of charge *via* the Internet at http://pubs.acs.org.

REFERENCES AND NOTES

1. Adrian, J. E.; Morselt, H. W.; Suss, R.; Barnert, S.; Kok, J. W.; Asgeirsdottir, S. A.; Ruiters, M. H.; Molema, G.; Kamps, J. A. Targeted SAINT-O-Somes for Improved Intracellular Delivery of siRNA and Cytotoxic Drugs into Endothelial Cells. *J. Controlled Release* **2010**, *144*, 341–349.
2. Ding, B. S.; Dziubla, T.; Shuvaev, V. V.; Muro, S.; Muzykantov, V. R. Advanced Drug Delivery Systems That Target the Vascular Endothelium. *Mol. Interventions* **2006**, *6*, 98–112.
3. Schmieder, A. H.; Caruthers, S. D.; Zhang, H.; Williams, T. A.; Robertson, J. D.; Wickline, S. A.; Lanza, G. M. Three-Dimensional MR Mapping of Angiogenesis with $\alpha5\beta1(\alpha\nu\beta3)$-Targeted Theranostic Nanoparticles in the MDA-MB-435 Xenograft Mouse Model. *FASEB J.* **2008**, *22*, 4179–4189.
4. Rosenbaugh, E. G.; Roat, J. W.; Gao, L.; Yang, R. F.; Manickam, D. S.; Yin, J. X.; Schultz, H. D.; Bronich, T. K.; Batrakova, E. V.; Kabanov, A. V.; *et al.* The Attenuation of Central Angiotensin II-Dependent Pressor Response and Intraneuronal Signaling by Intracarotid Injection of Nanoformulated Copper/Zinc Superoxide Dismutase. *Biomaterials* **2010**, *31*, 5218–5226.
5. Wood, K. C.; Azarin, S. M.; Arap, W.; Pasqualini, R.; Langer, R.; Hammond, P. T. Tumor-Targeted Gene Delivery Using Molecularly Engineered Hybrid Polymers Functionalized with a Tumor-Homing Peptide. *Bioconjugate Chem.* **2008**, *19*, 403–405.
6. Valadon, P.; Garnett, J. D.; Testa, J. E.; Bauerle, M.; Oh, P.; Schnitzer, J. E. Screening Phage Display Libraries for Organ-Specific Vascular Immunotargeting *in Vivo*. *Proc. Natl. Acad. Sci. U.S.A.* **2006**, *103*, 407–412.
7. Muzykantov, V. R.; Atochina, E. N.; Ischiropoulos, H.; Danilov, S. M.; Fisher, A. B. Immunotargeting of Antioxidant Enzyme to the Pulmonary Endothelium. *Proc. Natl. Acad. Sci. U.S.A.* **1996**, *93*, 5213–5218.
8. Pasqualini, R.; McDonald, D. M.; Arap, W. Vascular Targeting and Antigen Presentation. *Nat. Immunol.* **2001**, *2*, 567–568.
9. Muzykantov, V. R. Biomedical Aspects of Targeted Delivery of Drugs to Pulmonary Endothelium. *Expert Opin. Drug Delivery* **2005**, *2*, 909–926.
10. Danilov, S. M.; Gavrilyuk, V. D.; Franke, F. E.; Pauls, K.; Harshaw, D. W.; McDonald, T. D.; Miletich, D. J.; Muzykantov, V. R. Lung Uptake of Antibodies to Endothelial Antigens: Key Determinants of Vascular Immunotargeting. *Am. J. Physiol. Lung Cell Mol. Physiol.* **2001**, *280*, L1335–L1347.
11. Ding, B. S.; Hong, N.; Murciano, J. C.; Ganguly, K.; Gottstein, C.; Christofidou-Solomidou, M.; Albelda, S. M.; Fisher, A. B.; Cines, D. B.; Muzykantov, V. R. Prophylactic Thrombolysis by Thrombin-Activated Latent Prourokinase Targeted to PECAM-1 in the Pulmonary Vasculature. *Blood* **2008**, *111*, 1999–2006.
12. Muzykantov, V. R.; Christofidou-Solomidou, M.; Balyasnikova, I.; Harshaw, D. W.; Schultz, L.; Fisher, A. B.; Albelda, S. M. Streptavidin Facilitates Internalization and Pulmonary Targeting of an Anti-endothelial Cell Antibody (Platelet-Endothelial Cell Adhesion Molecule 1): A Strategy for Vascular Immunotargeting of Drugs. *Proc. Natl. Acad. Sci. U.S.A.* **1999**, *96*, 2379–2384.
13. Shuvaev, V. V.; Christofidou-Solomidou, M.; Bhora, F.; Laude, K.; Cai, H.; Dikalov, S.; Arguiri, E.; Solomides, C. C.; Albelda, S. M.; Harrison, D. G.; *et al.* Targeted Detoxification of Selected Reactive Oxygen Species in the Vascular Endothelium. *J. Pharmacol. Exp. Ther.* **2009**, *331*, 404–411.
14. Muro, S.; Garnacho, C.; Champion, J. A.; Leferovich, J.; Gajewski, C.; Schuchman, E. H.; Mitragotri, S.; Muzykantov, V. R. Control of Endothelial Targeting and Intracellular Delivery of Therapeutic Enzymes by Modulating the Size and Shape of ICAM-1-Targeted Carriers. *Mol. Ther.* **2008**, *16*, 1450–1458.
15. Maruyama, K.; Kennel, S. J.; Huang, L. Lipid Composition Is Important for Highly Efficient Target Binding and Retention of Immunoliposomes. *Proc. Natl. Acad. Sci. U.S.A.* **1990**, *87*, 5744–5748.
16. Ding, B. S.; Hong, N.; Christofidou-Solomidou, M.; Gottstein, C.; Albelda, S. M.; Cines, D. B.; Fisher, A. B.; Muzykantov, V. R. Anchoring Fusion Thrombomodulin to the Endothelial Lumen Protects Against Injury-Induced Lung Thrombosis and Inflammation. *Am. J. Respir. Crit. Care Med.* **2009**, *180*, 247–256.
17. Kozower, B. D.; Christofidou-Solomidou, M.; Sweitzer, T. D.; Muro, S.; Buerk, D. G.; Solomides, C. C.; Albelda, S. M.; Patterson, G. A.; Muzykantov, V. R. Immunotargeting of Catalase to the Pulmonary Endothelium Alleviates Oxidative Stress and Reduces Acute Lung Transplantation Injury. *Nat. Biotechnol.* **2003**, *21*, 392–398.
18. Dziubla, T. D.; Shuvaev, V. V.; Hong, N. K.; Hawkins, B. J.; Madesh, M.; Takano, H.; Simone, E.; Nakada, M. T.; Fisher, A.; Albelda, S. M.; *et al.* Endothelial Targeting of Semi-permeable Polymer Nanocarriers for Enzyme Therapies. *Biomaterials* **2008**, *29*, 215–227.
19. Muro, S.; Schuchman, E. H.; Muzykantov, V. R. Lysosomal Enzyme Delivery by ICAM-1-Targeted Nanocarriers Bypassing Glycosylation- and Clathrin-Dependent Endocytosis. *Mol. Ther.* **2006**, *13*, 135–141.
20. Shuvaev, V. V.; Han, J.; Yu, K. J.; Huang, S.; Hawkins, B. J.; Madesh, M.; Nakada, M.; Muzykantov, V. R. PECAM-Targeted Delivery of SOD Inhibits Endothelial Iinflammatory Response. *FASEB J.* **2011**, *25*, 348–357.
21. Kohane, D. S. Microparticles and Nanoparticles for Drug Delivery. *Biotechnol. Bioeng.* **2007**, *96*, 203–209.
22. Srivastava, S.; Santos, A.; Critchley, K.; Kim, K. S.; Podsiadlo, P.; Sun, K.; Lee, J.; Xu, C.; Lilly, G. D.; Glotzer, S. C.; *et al.* Light-Controlled Self-Assembly of Semiconductor Nanoparticles into Twisted Ribbons. *Science* **2010**, *327*, 1355–1359.
23. Shah, R. N.; Shah, N. A.; Del Rosario Lim, M. M.; Hsieh, C.; Nuber, G.; Stupp, S. I. Supramolecular Design of Self-Assembling Nanofibers for Cartilage Regeneration. *Proc. Natl. Acad. Sci. U.S.A.* **2010**, *107*, 3293–3298.
24. Poon, Z.; Lee, J. A.; Huang, S.; Prevost, R. J.; Hammond, P. T. Highly Stable, Ligand-Clustered "Patchy" Micelle Nanocarriers for Systemic Tumor Targeting. *Nanomedicine* **2011**, *7*, 201–209.
25. Gratton, S. E.; Ropp, P. A.; Pohlhaus, P. D.; Luft, J. C.; Madden, V. J.; Napier, M. E.; DeSimone, J. M. The Effect of Particle Design on Cellular Internalization Pathways. *Proc. Natl. Acad. Sci. U.S.A.* **2008**, *105*, 11613–11618.
26. Simone, E. A.; Dziubla, T. D.; Muzykantov, V. R. Polymeric Carriers: Role of Geometry in Drug Delivery. *Expert Opin. Drug Delivery* **2008**, *5*, 1283–1300.
27. Wang, Y.; Merkel, T. J.; Chen, K.; Fromen, C. A.; Betts, D. E.; DeSimone, J. M. Generation of a Library of Particles Having Controlled Sizes and Shapes *via* the Mechanical Elongation of Master Templates. *Langmuir* **2011**, *27*, 524–528.
28. Champion, J. A.; Mitragotri, S. Role of Target Geometry in Phagocytosis. *Proc. Natl. Acad. Sci. U.S.A.* **2006**, *103*, 4930–4934.
29. Geng, Y.; Dalhaimer, P.; Cai, S.; Tsai, R.; Tewari, M.; Minko, T.; Discher, D. E. Shape Effects of Filaments *versus* Spherical Particles in Flow and Drug Delivery. *Nat. Nanotechnol.* **2007**, *2*, 249–255.
30. Christian, D. A.; Tian, A.; Ellenbroek, W. G.; Levental, I.; Rajagopal, K.; Janmey, P. A.; Liu, A. J.; Baumgart, T.; Discher, D. E. Spotted Vesicles, Striped Micelles and Janus Assemblies Induced by Ligand Binding. *Nat. Mater.* **2009**, *8*, 843–849.
31. Simone, E. A.; Dziubla, T. D.; Discher, D. E.; Muzykantov, V. R. Filamentous Polymer Nanocarriers of Tunable Stiffness That Encapsulate the Therapeutic Enzyme Catalase. *Biomacromolecules* **2009**, *10*, 1324–1330.
32. Kennel, S. J.; Hotchkiss, J. A.; Rorvik, M. C.; Allison, D. P.; Foote, L. J. Rat Monoclonal Antibodies to Mouse Lung

Components for Analysis of Fibrosis. *Exp. Mol. Pathol.* **1987**, *47*, 110–124.
33. Rorvik, M. C.; Allison, D. P.; Hotchkiss, J. A.; Witschi, H. P.; Kennel, S. J. Antibodies to Mouse Lung Capillary Endothelium. *J. Histochem. Cytochem.* **1988**, *36*, 741–749.
34. Shuvaev, V. V.; Christofidou-Solomidou, M.; Scherpereel, A.; Simone, E.; Arguiri, E.; Tliba, S.; Pick, J.; Kennel, S.; Albelda, S. M.; Muzykantov, V. R. Factors Modulating the Delivery and Effect of Enzymatic Cargo Conjugated with Antibodies Targeted to the Pulmonary Endothelium. *J. Controlled Release* **2007**, *118*, 235–244.
35. Oh, P.; Li, Y.; Yu, J.; Durr, E.; Krasinska, K. M.; Carver, L. A.; Testa, J. E.; Schnitzer, J. E. Subtractive Proteomic Mapping of the Endothelial Surface in Lung and Solid Tumours for Tissue-Specific Therapy. *Nature* **2004**, *429*, 629–635.
36. Muro, S.; Wiewrodt, R.; Thomas, A.; Koniaris, L.; Albelda, S. M.; Muzykantov, V. R.; Koval, M. A Novel Endocytic Pathway Induced by Clustering Endothelial ICAM-1 or PECAM-1. *J. Cell. Sci.* **2003**, *116*, 1599–1609.
37. Shuvaev, V. V.; Tliba, S.; Pick, J.; Arguiri, E.; Christofidou-Solomidou, M.; Albelda, S. M.; Muzykantov, V. R. Modulation of Endothelial Targeting by Size of Antibody–Antioxidant Enzyme Conjugates. *J. Controlled Release* **2011**, *149*, 236–241.
38. Dalhaimer, P.; Engler, A. J.; Parthasarathy, R.; Discher, D. E. Targeted Worm Micelles. *Biomacromolecules* **2004**, *5*, 1714–1719.
39. Torchilin, V. P.; Levchenko, T. S.; Lukyanov, A. N.; Khaw, B. A.; Klibanov, A. L.; Rammohan, R.; Samokhin, G. P.; Whiteman, K. R. *p*-Nitrophenylcarbonyl-PEG-PE-Liposomes: Fast and Simple Attachment of Specific Ligands, Including Monoclonal Antibodies, to Distal Ends of PEG Chains *via p*-Nitrophenylcarbonyl Groups. *Biochim. Biophys. Acta* **2001**, *1511*, 397–411.
40. Scherpereel, A.; Rome, J. J.; Wiewrodt, R.; Watkins, S. C.; Harshaw, D. W.; Alder, S.; Christofidou-Solomidou, M.; Haut, E.; Murciano, J. C.; Nakada, M.; *et al.* Platelet-Endothelial Cell Adhesion Molecule-1-Directed Immunotargeting to Cardiopulmonary Vasculature. *J. Pharmacol. Exp. Ther.* **2002**, *300*, 777–786.